

Supporting Information

Novel redox bromide-ion additive hydrogel electrolyte for flexible zinc-ion hybrid supercapacitors with boosted energy density and controllable zinc deposition

Lu Han, Hailong Huang*, Junfeng Li, Xinlu Zhang, Zhongli Yang, Min Xu* and Likun Pan*

School of Physics and Materials Science & Shanghai Key Laboratory of Magnetic Resonance, East China Normal University, No. 500 Dongchuan Road, Shanghai 200241, P R China.

**Corresponding author:*

E-mail: huanghao3310774@163.com

Fax: +86 21 62234321; Tel: +86 21 62234132; E-mail: lkpan@phy.ecnu.edu.cn

Fax: +86 21 62233281; Tel: +86 21 62233263; E-mail: xumin@phy.ecnu.edu.cn

Experimental section

Characterizations

The Fourier transform infrared spectroscopy (FTIR) measurement was performed on Nicolet-Nexus 670 spectrophotometer at room temperature. The microstructure of the hydrogel was examined by scanning electron microscope (SEM, Hitachi S-4800). The mechanical performance of hydrogel was performed on the tensile machine (Instron 5967) at room temperature. For the tensile property, the sample was prepared as cylinder (diameter: 5 mm, height: 10 mm) and measured at a deformation rate of 25 mm min⁻¹ at 25 °C. For the compressive strength, the sample was prepared as cylinder (diameter: 20 mm, height: 20 mm) with an applied strain rate of 1 mm min⁻¹. The low-field nuclear magnetic resonance (L-NMR) was measured by NIUMAG NMRC12-010V-T at a resonance frequency of 21.56 MHz (0.5 T). The sample was put into the NMR cylindrical glass tubes to measure the relaxation time (T_2) using the Carr-Purcell-Meiboom-Gill sequence.

Electrochemical measurements

AC cathode was prepared by mixing 80 wt.% AC, 10 wt.% carbon black and 10 wt.% PVDF in an NMP solvent, and then coating the mixture onto graphite paper, which was dried at 60 °C in constant temperature oven. Typically, each working electrode has an exposed area of 1 × 1 cm² with a mass loading of 1 mg. Zn metal foil was directly used as anode, which should be polished with finegrained sandpaper to avoid being oxidized. AC//SA-Zn-Br//Zn BH-ZHS was assembled with SA-Zn-Br acting as a separator of cathode and anode. Cyclic

voltammetry (CV) and galvanostatic charge-discharge (GCD) tests were applied to evaluate the electrochemical behaviours of BH-ZHS using an electrochemical workstation (Autolab PGSTAT302N). The cycling stability measurement of BH-ZHS was carried out on a LAND battery-testing instrument at a sweep charge and discharge rate of 5 A g^{-1} for 5000 cycles.

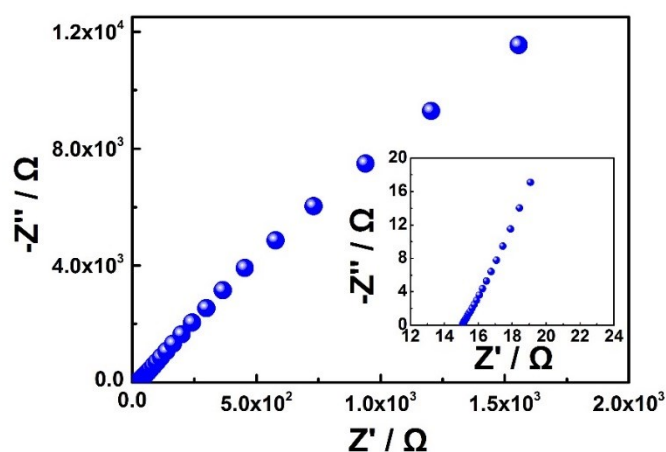


Fig. S1 Nyquist plot of SA-Zn hydrogel.

Electrochemical impedance spectroscopy (EIS) was measured using a two-electrode system (titanium foil// SA-Zn hydrogel //titanium foil) and the result is displayed in Fig. S1. The size of SA-Zn hydrogel is $1 \text{ cm} \times 1 \text{ cm} \times 0.5 \text{ cm}$, and its resistance is about $15.1 \text{ } \Omega$, as shown in the inset of Fig. S1. The ionic conductivity can be calculated by the following equation:

$$R = \rho \frac{l}{A} \quad (\text{S1})$$

$$\kappa = \frac{1}{\rho} \quad (\text{S2})$$

where R (Ω), l (m) and A (m^2) correspond to the resistance, thickness and area of SA-Zn hydrogel. The κ (S m^{-1}) and ρ ($\Omega \text{ m}^{-1}$) represent electrical conductivity and resistivity, respectively.

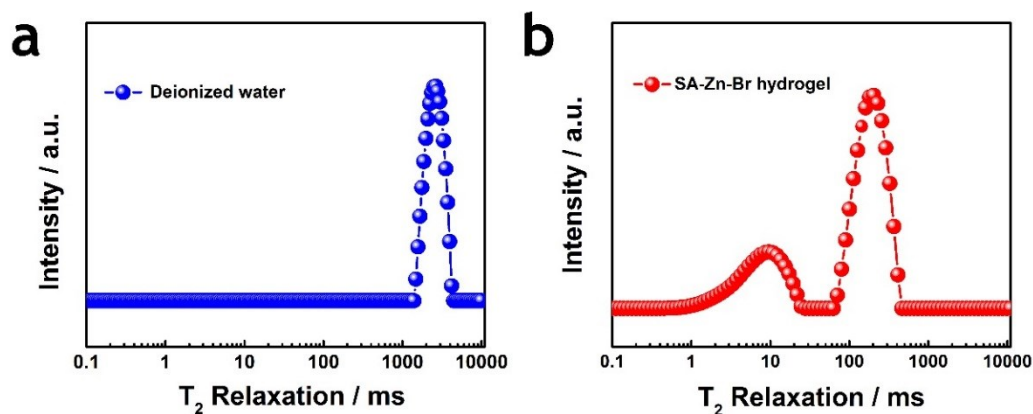


Fig. S2 The reciprocal of spin-spin relaxation time of (a) deionized water and (b) SA-Zn-Br hydrogel electrolyte. T_2 : (<10 ms), bond water; T_2 : (10-100 ms), intermediate water; T_2 : (>1000 ms), free water.¹

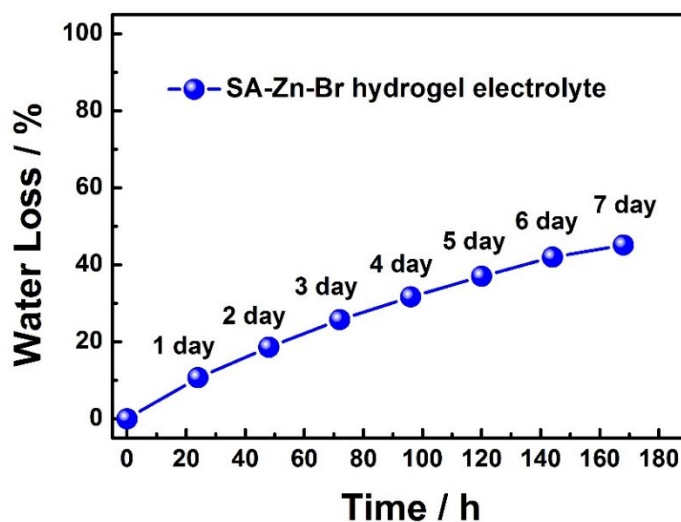


Fig. S3 Evolutions of water loss with time (one week=168 h) for SA-Zn hydrogel kept at room temperature.

In order to evaluate the accurate water loss of the hydrogel with time, its mass was recorded at every certain time (24 h) using an electronic scale, and the water loss rate (%) at time = i can be calculated by:

$$\text{Water Loss Rate} = \frac{\text{Mass (hydrogel, time = 0)} - \text{Mass (hydrogel, time = i)}}{\text{Mass (water, time = 0)}} \times 100\% \quad (\text{S3})$$

$$\text{Water Retention Rate} = 100\% - \text{Water Loss Rate} \quad (\text{S4})$$

where Mass (water, time = 0) is the mass of added water in prepared hydrogel.

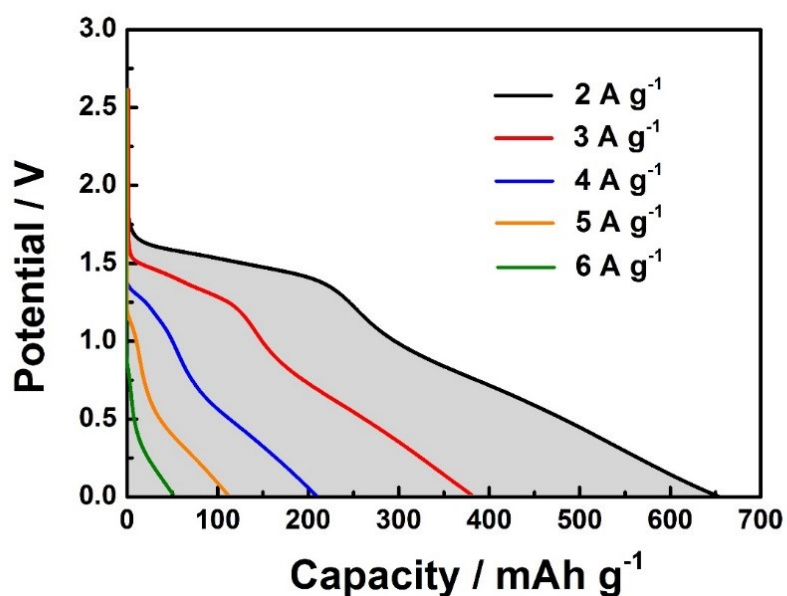


Fig. S4 Plots of integrating U (operating voltage / V) over Q (specific capacity / mAh g⁻¹) at various current densities (2-6 A g⁻¹) for calculating the energy density of BH-ZHS.

The specific energy density (E , Wh kg⁻¹) is the product of the specific capacity Q (mAh g⁻¹) based on the mass of activated carbon (AC) (about 1 mg cm⁻²) and the operating voltage U (V) in one full discharge cycle, and can be calculated by integrating U over Q : $E = \int U dQ$. Therefore, the area of zone (grey color) in Fig. S4 equals to the specific energy density.^{2,3} And the power density (P , W kg⁻¹) can be calculated as follows: $P = E/T$, T (h) corresponds to the discharge time.

Table S1 Comparison of electrochemical performances of BH-ZHS with the conventional ZHS reported in the literatures.

| Electrode materials | Specific capacity / capacitance | Electrolyte | Energy density (Wh kg ⁻¹) | Operating voltage window (V) | Ref. |
|---|---------------------------------|--|---------------------------------------|------------------------------|-----------|
| Zn//AC | 170 F g ⁻¹ | 1 M Zn (CF ₃ SO ₃) ₂ (organic) | 52.7 | 0-1.8 | [4] |
| Zn// porous carbon | 305 mAh g ⁻¹ | 2 M ZnSO ₄ +1 M Na ₂ SO ₄ (aqueous) | 118 | 0-1.8 | [5] |
| Zn//MXene-reduced graphene oxide aerogel | 128.6 F g ⁻¹ | 2 M ZnSO ₄ (aqueous) | 34.9 | 0.2-1.6 | [6] |
| Zn//graphene @ polyaniline | 154 mAh g ⁻¹ | 2 M ZnSO ₄ (aqueous) | 205 | 0.3-1.6 | [7] |
| Zn//AC | 121 mAh g ⁻¹ | 2 M ZnSO ₄ (aqueous) | 84 | 0.2-1.8 | [8] |
| Zn//AC | / | 2 M ZnSO ₄ (aqueous) | 94 | 0.2-1.8 | [9] |
| Zn//Hollow carbon spheres | 86.8 mAh g ⁻¹ | ZnSO ₄ polyacrylamide hydrogel electrolyte | 59.7 | 0.15-1.95 | [10] |
| Zn@Ti ₃ C ₂ // Ti ₃ C ₂ | 132 F g ⁻¹ | ZnSO ₄ gelatin electrolyte | / | 0.1-1.35 | [11] |
| Zn//AC | 654.8 mAh g ⁻¹ | redox SA-Zn-Br double network hydrogel electrolyte | 605 | 0-2.6 | This work |

References

- [1] Y. Li, X. Li, C. Chen, D. Zhao, Z. Su, G. Ma, R. Yu, *Carbohydr. Polym.* 2016, **151**, 1251-1260.

- [2] L. Dong, X. Ma, Y. Li, L. Zhao, W. Liu, J. Cheng, C. Xu, B. Li, Q.-H. Yang, F. Kang, *Energy Storage Mater.* 2018, **13**, 96-102.
- [3] L. Zhang, L. Chen, X. Zhou, Z. Liu, *Sci. Rep.* 2015, **5**, 18263.
- [4] H. Wang, M. Wang and Y. Tang, *Energy Storage Mater.*, 2018, **13**, 1-7.
- [5] P. Yu, Y. Zeng, Y. Zeng, H. Dong, H. Hu, Y. Liu, M. Zheng, Y. Xiao, X. Lu and Y. Liang, *Electrochim. Acta*, 2019, **327**, 134999
- [6] Q. Wang, S. Wang, X. Guo, L. Ruan, N. Wei, Y. Ma, J. Li, M. Wang, W. Li and W. Zeng, *Adv. Electron. Mater.*, 2019, **5**, 1900537.
- [7] J. Han, K. Wang, W. Liu, C. Li, X. Sun, X. Zhang, Y. An, S. Yi and Y. Ma, *Nanoscale*, 2018, **10**, 13083-13091.
- [8] L. Dong, X. Ma, Y. Li, L. Zhao, W. Liu, J. Cheng, C. Xu, B. Li, Q.-H. Yang and F. Kang, *Energy Storage Mater.*, 2018, **13**, 96-102.
- [9] L. He, Y. Liu, C. Li, D. Yang, W. Wang, W. Yan, W. Zhou, Z. Wu, L. Wang, Q. Huang, Y. Zhu, Y. Chen, L. Fu, X. Hou and Y. Wu, *ACS Appl. Energy Mater.*, 2019, **2**, 5835-5842.
- [10] S. Chen, L. Ma, K. Zhang, M. Kamruzzaman, C. Zhi and J. A. Zapien, *J. Mater. Chem. A*, 2019, **7**, 7784-7790.
- [11] Q. Yang, Z. Huang, X. Li, Z. Liu, H. Li, G. Liang, D. Wang, Q. Huang, S. Zhang, S. Chen and C. Zhi, *ACS Nano*, 2019, **13**, 8275-8283.